

# Epithelial Cell-Like Elasticity Modulates Actin-Dependent E-Cadherin Adhesion Organization

Mohamad Eftekharijoo,<sup>†</sup> Mazen Mezher,<sup>†</sup> Siddharth Chatterji, and Venkat Maruthamuthu\*Cite This: <https://doi.org/10.1021/acsbmaterials.2c00253>

Read Online

ACCESS |



Metrics &amp; More



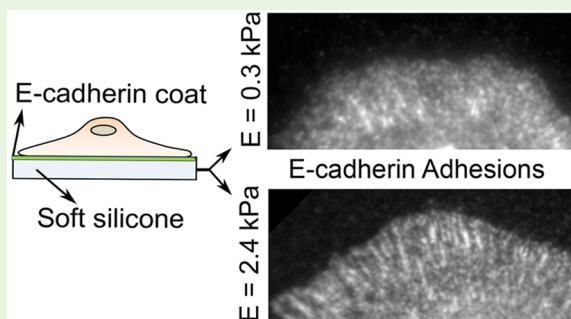
Article Recommendations



Supporting Information

**ABSTRACT:** E-cadherin adhesions are essential for cell-to-cell cohesion and mechanical coupling between epithelial cells and reside in a microenvironment that comprises the adjoining epithelial cells. While E-cadherin has been shown to be a mechanosensor, it is unknown if E-cadherin adhesions can differentially sense stiffness within the range of that of epithelial cells. A survey of literature shows that epithelial cells' Young's moduli of elasticity lie predominantly in the sub-kPa to few-kPa range, with cancer cells often being softer than noncancerous ones. Here, we devised oriented E-cadherin-coated soft silicone substrates with sub-kPa or few-kPa elasticity but with similar viscous moduli and found that E-cadherin adhesions differentially organize depending on the magnitude of epithelial cell-like elasticity. Our results show that the actin cytoskeleton organizes E-cadherin adhesions in two ways—by supporting irregularly shaped adhesions at localized regions of high actin density and linear shaped adhesions at the end of linear actin bundles. Linearly shaped E-cadherin adhesions associated with radially oriented actin—but not irregularly shaped E-cadherin adhesions associated with circumferential actin foci—were much more numerous on 2.4 kPa E-cadherin substrates compared to 0.3 kPa E-cadherin substrates. However, the total amount of E-cadherin in both types of adhesions taken together was similar on the 0.3 and 2.4 kPa E-cadherin substrates across many cells. Our results show how the distribution of E-cadherin adhesions, supported by actin density and architecture, is modulated by epithelial cell-like elasticity and have significant implications for disease states like carcinomas characterized by altered epithelial cell elasticity.

**KEYWORDS:** E-cadherin, adhesion, cell elasticity, actin, cell stiffness, mechanobiology, force



## INTRODUCTION

E-cadherin is a cardinal epithelial cell–cell adhesion molecule that is essential for proper morphogenesis as well as for the maintenance of the architecture of adult epithelial tissues.<sup>1,2</sup> At the microscale, E-cadherin adhesions are collectives of many *trans*-interacting E-cadherin *cis*-dimers/clusters from the surface of neighboring epithelial cells.<sup>3</sup> They form functional units that intimately couple to the underlying actin cytoskeleton to integrate the contractile and adhesive responses of epithelial cells.<sup>4–6</sup> Understanding both the biochemical and biophysical aspects of E-cadherin adhesions is essential to deciphering their role in larger cell collectives and tissues. Importantly, E-cadherin adhesions have been shown to be bonafide mechanosensors,<sup>7</sup> much like integrin-based adhesions.<sup>8</sup> Mechanosensitivity at the cell extracellular matrix (ECM)<sup>9</sup> and cell–cell contacts<sup>10–12</sup> is of fundamental relevance to morphogenesis,<sup>13</sup> maintenance of tissue architecture, as well as disease progression.<sup>14</sup> While integrin-based adhesions are known to be sensitive to elasticity within the range of that of the ECM,<sup>8</sup> it is unclear if E-cadherin-based adhesions can differentially sense elasticity within the range of that of epithelial cells that enclose them.

While potential sensing of cell-like elasticity by E-cadherin adhesions may be relevant for processes like wound healing,<sup>15</sup> it is especially relevant in the context of cancer progression. First, E-cadherin is a well-known tumor suppressor but is continued to be expressed in many types of cancers.<sup>16</sup> It has also been shown that the modulation of E-cadherin adhesion may play a key role in cancer progression.<sup>17</sup> In this context, it has been proposed<sup>17</sup> that inside-out signaling can modulate E-cadherin adhesions. Since human epithelial cancer cells are often softer than normal cells,<sup>18</sup> it is also possible that E-cadherin mechanosensing of cell elasticity may be at play. We noticed that many, although not all, studies that compared normal or benign human epithelial cells with cancerous ones from the same tissue of origin reported a similar trend: the Young's modulus was 2 kPa for normal vs 0.5 kPa for cancer cells from lungs,<sup>19</sup> 2 kPa for normal vs 0.5 kPa for cancer cells

Received: March 3, 2022

Accepted: April 18, 2022

from breasts,<sup>19</sup> 2.5 kPa for normal vs 0.5–1.1 kPa for cancer cells from ovaries,<sup>20</sup> 2.2 kPa for normal vs 1.4 for cancer cells from thyroid,<sup>21</sup> and 2.8 kPa for normal vs 0.3–1.4 kPa for cancer cells from prostate.<sup>22</sup> Thus, potential E-cadherin sensing of elasticity in the sub-kPa to few-kPa range is of physiological relevance, and testing for it requires an E-cadherin-specific soft substrate in this range of elasticity.

E-cadherin adhesions are typically studied using epithelial islands or monolayers that have extensive cell–cell contacts. However, E-cadherin adhesions at epithelial cell–cell contacts exist among a complex milieu of other cell–cell adhesion systems. Epithelial cell–cell contacts consist of several types of cell–cell junctions including tight junctions, adherens junctions, desmosomes, and gap junctions.<sup>23</sup> Adherens junctions themselves consist of not only E-cadherin adhesions but also other types of cell–cell adhesions such as those mediated by nectins. To enable the specific probing of cadherin, several groups have utilized cadherin-coated surfaces.<sup>24–28</sup> Glass surfaces coated with the extracellular region of E-cadherin fused to the Fc region (E-cadherin-Fc) have especially been used to study biochemical events initiated specifically by E-cadherin adhesion.<sup>29</sup> E-cadherin surfaces also enable easier imaging of adhesions in a 2D plane compared to native epithelial cell–cell contacts that have a more complex topology. In the latter, several types of cell–cell adhesions at epithelial cell–cell junctions are regulated by F-actin. In particular, E-cadherin is very closely regulated by the actin cytoskeleton,<sup>30</sup> with the archetypical apical band of E-cadherin around epithelial cells closely apposed to a corresponding belt of actin cytoskeleton.<sup>1</sup> E-cadherin substrates that are not only flat but also soft can enable us to observe how the actin cytoskeleton is coupled to discrete E-cadherin adhesions at an interface with epithelial cell-like elasticity. In particular, one can potentially ascertain the contributions of local high actin density and specific actin architecture toward supporting E-cadherin adhesions.

Flexible E-cadherin-coated substrates have specifically been used recently to understand E-cadherin mechanobiology.<sup>31,32</sup> It has been shown that E-cadherin adhesions can distinguish between elastic moduli within the tens of kPa range<sup>31</sup> (similar to N-cadherin<sup>33</sup>) as well as between kPa and MPa elastic moduli.<sup>32</sup> Importantly, however, it has not been addressed whether E-cadherin adhesions can differentially sense elasticity within the range of that of epithelial cells, i.e., in the sub-kPa to few-kPa range.<sup>18</sup> Furthermore, prior studies that used E-cadherin-coated surfaces to study E-cadherin mechanosensitivity<sup>31,32</sup> have not reported on the formation of discrete E-cadherin adhesions corresponding to this crucially relevant range of elasticity. Here, we first developed a biomimetic E-cadherin soft substrate by modifying prior approaches and then proceeded to employ it in answering the questions of (i) whether E-cadherin adhesion formation depends on the sensing of epithelial cell-like stiffness and (ii) how the actin cytoskeleton supports different types of E-cadherin adhesions on such cell-like soft microenvironments.

## MATERIALS AND METHODS

**Cell Culture.** Human colon epithelial cells (C2BBE, a subclone of Caco-2) were cultured overnight in Dulbecco's modified Eagle's medium (Corning Inc., Corning, NY) supplemented with L-glutamine, sodium pyruvate, 1% penicillin/streptomycin, and 10% fetal bovine serum (Corning Inc., Corning, NY) under 5% CO<sub>2</sub> at 37 °C. Before each experiment, cells were detached from cell culture

dishes using a trypsin-free chelator-based cell dissociation reagent (Versene, Thermo Fisher Scientific, Waltham, MA). The cells were seeded on samples in the same media as above, but without serum, for 2 h under 5% CO<sub>2</sub> at 37 °C.

**Biomimetic E-Cadherin Soft Substrate Preparation.** Soft silicone (GEL8100, NuSil Silicone Technologies, Carpinteria, CA, USA) was prepared by mixing the base and cross-linker components (labeled A and B) in the ratio 2:3 or 2:7 by weight. The storage and loss shear moduli of each formulation was characterized using an HR-2 Discovery rheometer (TA Instruments, New Castle, DE) in a parallel plate geometry. To prepare the substrates, about 100  $\mu$ L of soft silicone was first pipetted onto a 22 mm  $\times$  22 mm glass coverslip and cured for 1 h at 100 °C on a hot plate. The substrate was then exposed to 305 nm UV light (UVP cross-linker, Analytik Jena AG, Upland, CA) for 5 min. Protein A (Prospec, Rehovot, Israel) was then coupled to the substrate by incubation with an aqueous solution of 0.2 mg/mL protein A, 10 mg/mL EDC (1-ethyl-3-(3-dimethylamino-propyl) carbodiimide hydrochloride), and 5 mg/mL sulfo-NHS (*N*-hydroxysulfosuccinimide) for 1 h at room temperature. After washing with PBS (with calcium), the substrate was incubated with 0.1 mg/mL recombinant E-cadherin-Fc for 2 h (Sino Biological, Beijing, China). Afterwards, the sample was washed with PBS (with calcium) and incubated with 1 mg/mL Fc fragment (Jackson ImmunoResearch, West Grove, PA) for 1 h. The sample was again washed with PBS (with calcium) before cell plating.

**Immunofluorescence, Drug Treatment and Imaging.** Cells were permeabilized and fixed in buffer C (10 mM MES (2-morpholinoethanesulfonic acid), 3 mM MgCl<sub>2</sub>, and 138 mM KCl (pH 6.8) with 4% paraformaldehyde, 1.5% (w/v) bovine serum albumin, and 0.5% (v/v) Triton-X for 15 min. The cells were incubated overnight at 4 °C with primary antibodies and for 1 h at room temperature with secondary antibodies. Primary antibodies used were anti- $\beta$ -catenin (Clone 14, 610,154, BD Biosciences, San Jose, CA), anti-paxillin (Y113, ab32084, Abcam, Cambridge, UK), anti-phosphomyosin Light Chain 2 (Ser 19) (3671S, Cell Signaling Technology, Danvers, MA), and anti-E-cadherin (DECMA-1, sc-59778, Santa Cruz Biotechnology, Dallas, TX and CM1681, ECM Biosciences, Versailles, KY). Alexa Fluor 488-conjugated phalloidin was from Thermo Fisher Scientific, Waltham, MA, and DAPI was from Biotium, Hayward, CA. Secondary antibodies were from Jackson ImmunoResearch, West Grove, PA. Jaspilkinolide (used at 1 nM for 1 h) and SMIFH2 (used at 20  $\mu$ M for 2 h) were from MilliporeSigma, Burlington, MA. All images were taken using a Leica DMi8 epifluorescence microscope (Leica Microsystems, Buffalo Grove, IL) with 10 $\times$ , 20 $\times$ , or 40 $\times$  objectives and a Clara cooled CCD camera (Andor Technology, Belfast, Northern Ireland).

**Image Analysis.** To compare E-cadherin coating densities on the silicone surfaces, we used ImageJ<sup>34</sup> to extract the mean intensity values of the regions with deposited E-cadherin (as immunostained with anti-E-cadherin antibody DECMA-1). At least 13 regions with a cumulative area of  $\sim 5 \times 10^5 \mu\text{m}^2$  were included across two independent samples for each case. For E-cadherin adhesion analysis, discrete E-cadherin adhesions  $\sim 0.5 \mu\text{m}^2$  or larger were manually segmented using CellProfiler (Version 3.1.9),<sup>35</sup> using a Wacom Intuos pen tablet. Individual adhesion intensity and shape features were also extracted using CellProfiler. The eccentricity of an adhesion was obtained by first fitting an ellipse with the same second moment as the adhesion and then computing the ratio of the distance between the foci of the ellipse and its major axis length.

**Scanning Electron Microscopy.** To perform scanning electron microscopy (SEM) imaging, the GEL8100 2:3 and 2:7 silicone substrates (on glass coverslips) were coated and imaged using established procedures—briefly, the substrates were first coated with a thin layer of a gold–palladium alloy using a Polaron E5100 Series II sputter coater under an atmosphere of argon at less than 0.1 mbar. SEM imaging was performed with a Jeol JSM-6060LV scanning electron microscope.

**Statistical Analysis.** A two-tailed Student's *t* test was used with substrate cadherin intensity and cell area data. MATLAB (Math-

Works, Natick, MA) or Excel (Microsoft, Redmond, WA) was used to carry out the statistical analysis.

## RESULTS AND DISCUSSION

In order to observe and study E-cadherin adhesions free from other cell–cell adhesion systems, we first used glass substrates with oriented, immobilized Fc-tagged E-cadherin—based on earlier E-cadherin biophysical<sup>36</sup> and biochemical<sup>37</sup> studies (Figure 1A). The substrate was first coated with protein A, and

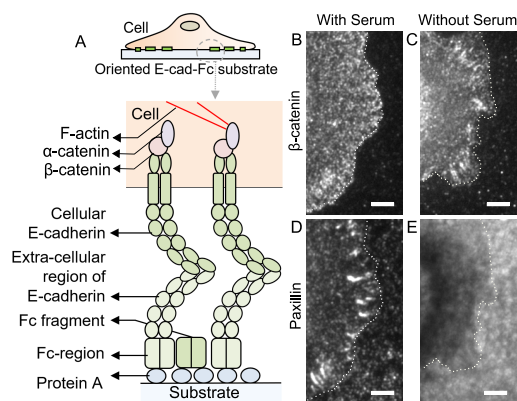


**Figure 1.** Oriented immobilized E-cadherin surface as a biomimetic “cell–cell” interface to enable E-cadherin adhesions and avoid focal adhesions. (A) Schematic depiction of the oriented immobilized E-cadherin substrate with an adherent cell. (B–E) Immunofluorescence images of C2BBE cells on glass E-cadherin substrates stained for  $\beta$ -catenin (B, C) and paxillin (D, E). In the presence of serum (B, D), E-cadherin adhesions (marked by  $\beta$ -catenin, (B)) are not well developed as prominent focal adhesions (marked by paxillin, (D)) form. In the absence of serum (C, E), E-cadherin adhesions (marked by  $\beta$ -catenin, (C)) are well developed as focal adhesions (marked by paxillin, (E)) are avoided. Cell edges are marked with dotted lines in (B–E). All scale bars are 5  $\mu$ m.

then E-cadherin was immobilized onto protein A (Figure 1A). We then plated human epithelial (C2BBE) cells on this substrate in complete cell culture medium with serum. We found that the cells adhered and spread well. We then used immunofluorescence to check the formation of E-cadherin adhesions, marked by  $\beta$ -catenin (since  $\beta$ -catenin binds to the cytoplasmic region of E-cadherin at a 1:1 stoichiometric ratio<sup>38</sup>) as well as focal adhesions (marked by paxillin). To

unambiguously attribute cell response to E-cadherin adhesion, we wanted to preclude the formation of focal adhesions. However, when plated in normal cell culture medium with serum, prominent focal adhesions rather than E-cadherin adhesions were present in all cells (Figure 1B,D). The use of integrin blocking antibodies used previously<sup>39</sup> did not prove successful for us. Including a blocking step with bovine serum albumin (BSA) did not preclude focal adhesion formation either (Figure S1). We reasoned that the extracellular matrix components present in the serum could be contributing to the formation of (in this context, unwanted) focal adhesions. We then plated the cells in serum-free media and found that focal adhesion formation was considerably reduced with a majority of cells that did not form any focal adhesions (Figure 1C,E). Only cells with E-cadherin adhesions and no focal adhesions (as checked with each cell by immunofluorescence) were considered for all data and analyses that follow. Serum-free media did not adversely affect cells (as observed by microscopy) for the timescales considered in this work (Figure S2).

One of the broad questions we were interested in was whether E-cadherin adhesions can sense and be affected by an elastic microenvironment that mimics the epithelial cells that enclose them. E-cadherin adhesions reside on the surface of epithelial cells in close proximity to the cell cortex. Thus, we reasoned that values of epithelial cell stiffness reported in literature using methods such as atomic force microscopy would be most relevant to E-cadherin mechanosensing as opposed to methods that measure the elasticity deep in the cytoplasm that do not involve contributions from the cell cortex.<sup>40</sup> A survey<sup>18</sup> of several studies<sup>19–22,41–46</sup> that used atomic force microscopy to measure the elasticity of normal and cancer human epithelial cells of same tissue origin shows (Figure 2A) that (i) human epithelial cell stiffness lies in the sub-kPa to few-kPa range and (ii) cancer cell stiffness is typically lower than that of normal cells. It has been previously shown that E-cadherin adhesions can sense applied forces<sup>11,47</sup> as well as tens of kPa stiffness.<sup>31</sup> Considering the overall distribution of human epithelial cell stiffness (normal as well as cancerous) in Figure 2A, we asked whether E-cadherin adhesions may differentially sense elasticity within this range. To attain this elasticity range, we tested soft silicones of various compositions and came up with ones (Figure 2B,C) that had Young’s moduli of sub-kPa (0.3 kPa) and few-kPa (2.4 kPa)

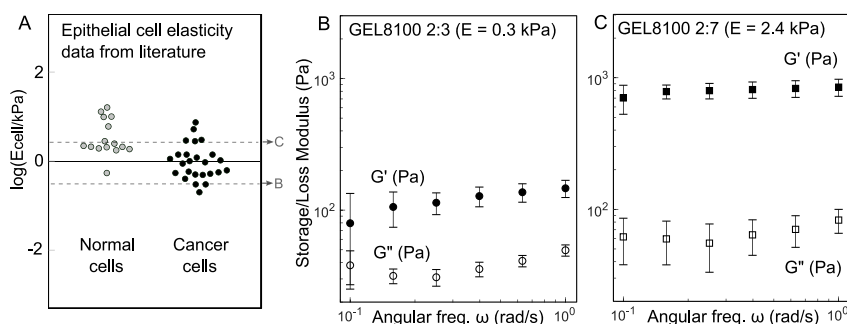


**Figure 2.** Silicone substrates with epithelial cell-like elasticity. (A) Young’s moduli of various human normal/benign and cancer epithelial cells ( $E_{\text{cell}}$ ) reported in literature<sup>19–22,41–46</sup> (Table S1) with  $E_{\text{cell}}$  in kPa. Note that the line at  $\text{Log}(E_{\text{cell}}/\text{kPa}) = 0$  corresponds to  $E_{\text{cell}}$  of 1 kPa. Dotted lines correspond to the Young’s moduli of the soft silicones in (B) and (C). (B, C) Rheology data of 2:3 (B) and 2:7 (C) GEL8100 soft silicone corresponding to Young’s moduli ( $E$ ) of 0.3 and 2.4 kPa, respectively. The storage ( $G'$ ) and loss ( $G''$ ) moduli of the soft silicones are shown as a function of angular frequency. Each data point is the mean  $\pm$  SD from three independent experiments. For incompressible soft silicone,  $E \approx 3G'_{\text{avg}}$  with  $G'_{\text{avg}}$  being the average of  $G'$  for  $\omega = 0.1$  to 1 rad/s.



magnitude while simultaneously having lower loss moduli (viscous component) of similar magnitude (tens of Pa) for either soft silicone (Figure 2B,C) (Note that  $G' = E/2(1 + \nu)$ ,<sup>48</sup> and since soft silicone is nearly incompressible,<sup>49,50</sup>  $\nu \approx 0.5$ . Thus,  $E \approx 3G'$ , where  $G'$  is the storage modulus or elastic component). Notably, these substrates have a loss modulus that is a fraction ( $\sim 0.1$ – $0.5$ ) of the storage modulus, similar to that reported for epithelial cells previously.<sup>51</sup> We then checked the roughness of the sub-kPa and few-kPa substrates using scanning electron microscopy (SEM). We found that both substrates were very smooth as imaged using SEM (Figure S3), implying a roughness scale of less than a few nm—the resolution limit of SEM). This was consistent with previous results with SEM imaging of silicone surfaces.<sup>52,53</sup>

The soft silicone was first coated with protein A (using EDC/sulfo-NHS chemistry), and then E-cadherin was immobilized onto protein A (as in Figure 1A). Importantly, a similar strategy was shown recently to mimic lateral E-cadherin-based cell–cell junctions effectively.<sup>54</sup> Using immunofluorescence, we first checked that the density of E-cadherin on the 0.3 and 2.4 kPa soft silicone substrates were similar (as shown in Figure S4; data from two independent samples for each substrate). We first noted that the cell spread area on the 0.3 and 2.4 kPa E-cadherin substrates were similar ( $1520 \pm 610$  and  $1470 \pm 450 \mu\text{m}^2$ , respectively;  $p = 0.45$  for 116 cells (0.3 kPa) and 145 cells (2.4 kPa) pooled from eight independent experiments) unlike in studies where higher elasticity values were considered.<sup>31,32</sup> The cells on both 0.3 and 2.4 kPa E-cadherin substrates displayed a “background” of diffraction-limited nascent E-cadherin adhesions throughout as well as larger discrete E-cadherin adhesions of around  $>0.5 \mu\text{m}^2$  (referred to simply as E-cadherin adhesions henceforth).

Two kinds of E-cadherin adhesions were observed via immunofluorescence (Figure 3B–E): adhesions associated with the ends of radially oriented F-actin structures (Figure 3B,D) and adhesions associated with actin foci along circumferential F-actin structures (Figure 3C,E). Since the former were often linearly shaped and the latter were often irregularly shaped, these two types of observed E-cadherin adhesions are henceforth referred to as linear and irregular adhesions (also see Figure S5; quantitative shape characterization of these adhesions detailed further below). The absence of focal adhesions, as marked by paxillin, is also evident in the corresponding images in Figure S6. The radial actin bundles (reminiscent of dorsal stress fibers<sup>55</sup> for cells adherent on ECM), with which linear adhesions were associated, also appeared well-integrated with circumferentially oriented actin bundles (Figure 3B,D) (the latter reminiscent of transverse arcs<sup>55</sup> for cells adherent on ECM). The actin foci along circumferentially oriented actin structures, with which irregular adhesions were associated, were micrometer-scale regions of high F-actin intensity (Figure 3C,E), and such foci are not typically observed for cell adhesion to the ECM. Both linear and irregular adhesions were largely spatially segregated from each other and present in different cells to different extents based on the prevalence of radial actin or actin foci along circumferentially oriented actin structures. Occasionally, they were also present closer to each other (Figure S7). To validate the use of  $\beta$ -catenin as a marker of E-cadherin adhesions, we also stained E-cadherin with an antibody directed against its cytoplasmic domain. This confirmed the presence of both irregular and linear E-cadherin adhesions as shown in Figure S8. Thus, we continued to use  $\beta$ -catenin as a marker of E-

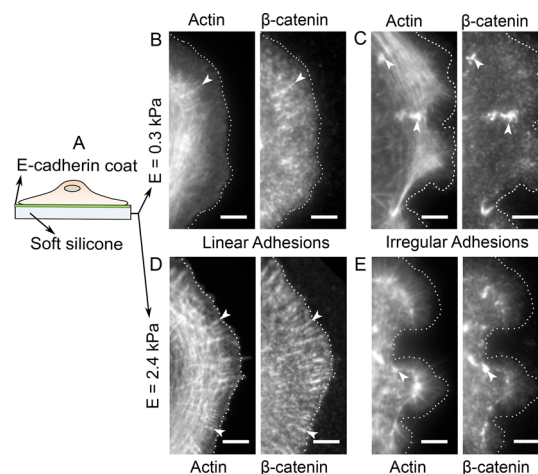


**Figure 3.** Actin-associated E-cadherin adhesion morphologies on sub-kPa and few-kPa E-cadherin substrates. (A) Schematic depiction of an epithelial cell adherent on an E-cadherin-coated soft silicone substrate. (B–E) Immunofluorescence images of C2BBE epithelial cells adherent on 0.3 kPa (B, C) or 2.4 kPa (D, E) E-cadherin substrates stained with phalloidin (to mark actin) and  $\beta$ -catenin (to mark E-cadherin adhesions). Linearly shaped radial actin-associated E-cadherin adhesions (B, D) and irregularly shaped circumferential actin foci-associated E-cadherin adhesions (C, E) are shown for both substrates. Arrow heads in the actin images indicate representative radial actin or the associated linear E-cadherin adhesions (B, D) as well as representative circumferential actin foci and the associated irregularly shaped E-cadherin adhesions (C, E). Cell edges are marked with dotted lines in (B–E). All scale bars are  $5 \mu\text{m}$ .

cadherin adhesions as it yielded a stain with higher contrast (lower background).

We segmented the E-cadherin adhesions using CellProfiler<sup>35</sup> and determined the number, shape, and intensity of E-cadherin adhesions of either kind on the 0.3 and 2.4 kPa substrates (also see Figure S9). The eccentricities (shape factors) of the linear adhesions on the 0.3 and 2.4 kPa substrates were  $0.92 \pm 0.04$  and  $0.91 \pm 0.06$ , respectively (insets in Figure 4A,C). Note that the eccentricity of a line is 1, whereas that of a circle is 0, showing that the linear adhesions were indeed quite linearly shaped. In contrast, the eccentricities of the irregular adhesions on 0.3 and 2.4 kPa substrates were lower and more broadly distributed ( $0.78 \pm 0.16$  and  $0.79 \pm 0.15$ , respectively; insets in Figure 4B,D). Overall, over twice as many E-cadherin adhesions formed on the 2.4 kPa substrate when compared to the 0.3 kPa substrate, in a similar number of cells (58 cells on the 0.3 kPa substrate and 59 cells on the 2.4 kPa substrate; pooled from three independent samples each). When resolved into linear and irregular adhesions, we found that  $\sim 5\times$  as many linear adhesions formed on the few-kPa substrate as the sub-kPa substrate (Figure 4A,C), whereas  $\sim 2\times$  as many irregular adhesions formed on the sub-kPa substrate as the few-kPa substrate (Figure 4B,D). This shows that E-cadherin adhesions can differentially sense sub-kPa vs few-kPa elasticity and organize differently in response. Notably, when we integrated the E-cadherin intensity in all the adhesions (both linear and irregular) across a similar number of cells on either substrate, we found that the total E-cadherin levels in all adhesions together were similar for the 0.3 and 2.4 kPa substrate (Figure 4E; even though there are way more linear adhesions on the few-kPa substrate, there are more irregular adhesions on the sub-kPa substrate, and since irregular adhesions are larger, they

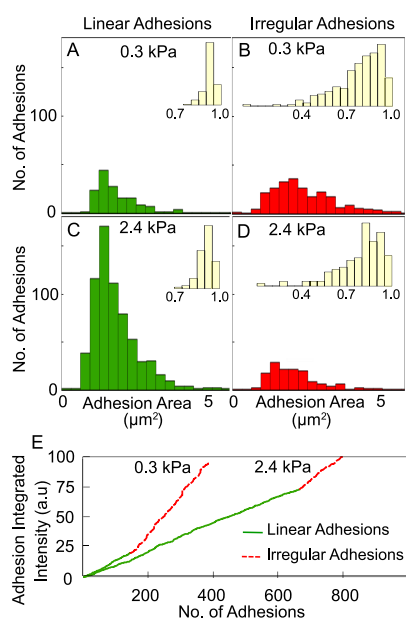


**Figure 4.** E-cadherin adhesion distribution depends on epithelial cell-like elasticity. (A–D) E-cadherin adhesion number versus area for linearly shaped radial actin-associated adhesions (A, C) and irregularly shaped circumferential actin foci-associated adhesions (B, D) as a function of epithelial cell-like 0.3 kPa (A, B) or 2.4 kPa (C, D) E-cadherin substrate elasticity. Inset (A–D): E-cadherin adhesion number versus eccentricity for linear (A, C) and irregular (B, D) adhesions. (E) Sum of the integrated intensity of all linear (green, solid) and irregular (red, dashed) E-cadherin adhesions on 0.3 and 2.4 kPa E-cadherin substrates. Data pooled from three independent experiments, with a total of 58 cells at 0.3 kPa and 59 cells at 2.4 kPa.

account for a disproportionately greater amount of integrated intensity than linear adhesions). This suggests that, overall, about the same level of E-cadherin is distributed in adhesions in different ways in response to the sub-kPa and few-kPa elastic E-cadherin substrates.

Finally, we wanted to ascertain the mechanisms by which the actin cytoskeleton may be supporting irregular and linear E-cadherin adhesions. We first tested whether the circumferential actin foci are localized regions of high contractility by testing for the presence of phosphomyosin. Irregular adhesions (Figure 5A), which were colocalized with actin foci (Figure 5B), did not typically show colocalization of phosphomyosin (Figure 5C), as is also evident in the line scan profiles in Figure 5D. Therefore, we then hypothesized that at circumferential actin foci, the high local actin density may itself support the localization of E-cadherin adhesion. To test this, we treated cells on E-cadherin soft substrates with 1 nM jasplakinolide, an inducer of actin polymerization and stabilization.<sup>56,57</sup> Since a dynamic actin cytoskeleton is essential for proper cell form, we observed that jasplakinolide treatment over many hours led to cell detachment over time (data not shown). At shorter treatment times (1 h), however, when cells stayed adhered and spread, we noticed that some cells displayed large actin foci (Figure 5E), which was somewhat an expected effect of jasplakinolide.<sup>58</sup> These large actin foci also supported irregularly shaped E-cadherin adhesions (Figure 5F,G) that were among the largest irregular adhesions we observed. A similar effect was obtained upon jasplakinolide treatment of cells on the sub-kPa E-cadherin substrate as well (Figure S10A,B). These results suggested that local high actin density

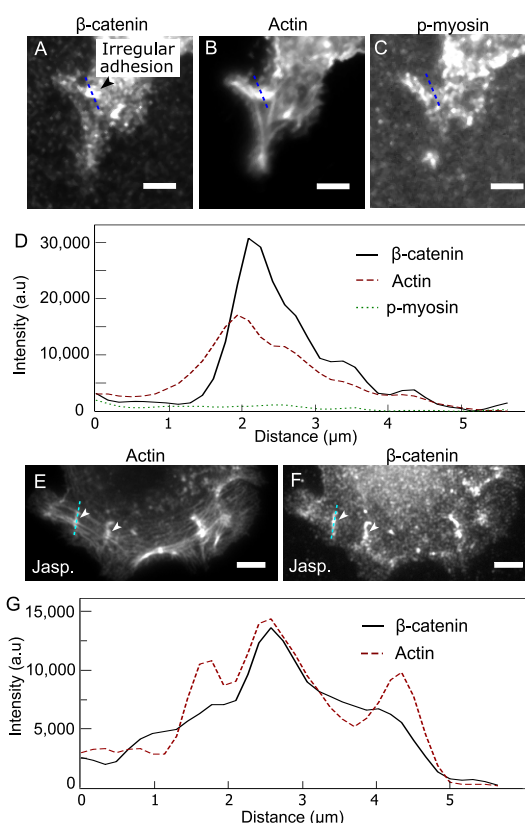


**Figure 5.** High local actin density supports irregular E-cadherin adhesions on cell-like soft E-cadherin substrates. (A–C) Immunofluorescence images of C2BBE cells on 2.4 kPa E-cadherin substrates stained for actin (A),  $\beta$ -catenin (B) and phospho-myosin (phosphoserine 19, light chain) (C). One of two visible irregular adhesions indicated with a black arrow head in (A) and blue dotted lines indicate scan lines whose intensity profiles are displayed in (D). (D) Line scans of  $\beta$ -catenin, actin, and phospho-myosin intensity for the dashed lines indicated in (A–C). (E, F) Immunofluorescence images of C2BBE cells on 2.4 kPa E-cadherin substrates treated with 1 nM jasplakinolide stained for actin (E) and  $\beta$ -catenin (F). Two large visible irregular adhesions indicated with white arrow heads in (E, F) and cyan dotted lines indicate scan lines whose intensity profiles are displayed in (G). (G) Line scans of actin and  $\beta$ -catenin intensity for the dashed lines indicated in (E, F). All scale bars are 5  $\mu$ m.

was the main driver behind the formation of irregular E-cadherin adhesions. Treatment with blebbistatin (20  $\mu$ M)<sup>59</sup> did not abrogate irregular adhesions associated with circumferential actin foci (Figure S11A,B), consistent with local actin density, rather than contractility, supporting these adhesions. In contrast, linear adhesions were no longer supported after blebbistatin treatment (Figure S11C,D).

With regard to the linear actin adhesions, the linear architecture of the associated contractile actin bundle was also evidently important. Thus, we hypothesized that formins, known nucleators of linear actin filaments,<sup>60</sup> may be necessary. Treatment with 20  $\mu$ M SMIFH2, a pan-formin inhibitor,<sup>61</sup> suppressed the presence of radially oriented linear actin structures and linear E-cadherin adhesions as well (Figure 6). Similar results were obtained upon SMIFH2 treatment of cells on the sub-kPa E-cadherin substrate as well (Figure S10C,D). This is consistent with the known role of formins in maintaining E-cadherin adhesions at cell–cell contacts.<sup>62</sup> It is worth noting that we used a relatively low concentration of

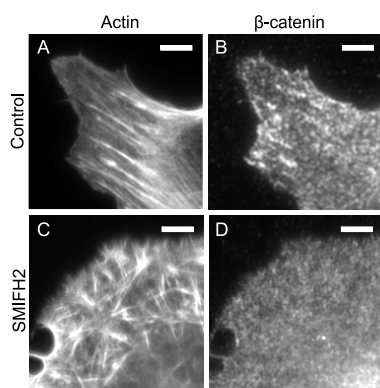


**Figure 6.** Formin activity is necessary for linear E-cadherin adhesions on cell-like soft E-cadherin substrates. (A–D) Immunofluorescence images of C2BBE cells on 2.4 kPa E-cadherin substrates treated with DMSO (A, B) or 20  $\mu$ M SMIFH2 (C, D), stained for actin (A, C) and  $\beta$ -catenin (B, D). All scale bars are 5  $\mu$ m.

SMIFH2 here since it has been shown to especially have pleiotropic effects<sup>63</sup> at higher concentrations.

## CONCLUSIONS

In this report, we devised biomimetic E-cadherin soft substrates with epithelial cell-like elasticities and showed that discrete E-cadherin adhesions are observed on cell-like soft E-cadherin substrates (unlike prior reports that either did not observe well-formed discrete adhesions<sup>31</sup> or used pillars with limited cross-sectional area<sup>32</sup>). Crucially, the amount of E-cadherin adhesions formed is different on sub-kPa and few-kPa substrates, and since only E-cadherin-based adhesions link the cell to the substrate, this involves E-cadherin-based sensing of substrate stiffness leading to the response of altered E-cadherin organization. It will be interesting to identify the extent to which various cellular factors (such as Rho GTPases and actin binding proteins) facilitate this specific effect of micro-environmental elasticity on E-cadherin adhesion organization. The enhanced formation of linear E-cadherin adhesions at higher cell-like stiffness as well as the necessity of formin for proper formation of these adhesions both point to the possibility of enhanced RhoA activation at E-cadherin adhesions in response to increase in cell stiffness.<sup>64,65</sup> E-cadherin sensing of epithelial cell-like elasticity may have implications in various physiological contexts where epithelial cell stiffness changes, such as during wound healing.<sup>15</sup> In the context of cancer mechanobiology, it is possible that softening of cells during cancer progression may decrease the level of E-cadherin adhesion and cell–cell contact stability. In our study, we also showed that the actin cytoskeleton supports E-cadherin adhesions (at cell-like microenvironmental stiffness) in two ways (local high density and linear architecture), corresponding to the two types of E-cadherin adhesions we observed (on both sub-kPa and few-kPa substrates). Based on our results, we propose that the apical circumferential actin belt harnesses both its high local density and linear architecture to support the associated E-cadherin adhesion belt at cell–cell junctions. E-cadherin adhesions serve complex roles—organizing cell–cell junctions, mechanically coupling neighboring cell cortices, maintaining cell polarity, and influencing a myriad of signaling pathways. We propose that E-cadherin sensing of epithelial cell-like stiffness may be an additional key role of these versatile adhesions.

## ASSOCIATED CONTENT

### Supporting Information

The Supporting Information is available free of charge at <https://pubs.acs.org/doi/10.1021/acsbmaterials.2c00253>.

(Figure S1) Blocking with BSA; (Figure S2) cell viability in serum absence; (Figure S3) SEM images; (Figure S4) E-cadherin surface intensity; (Figure S5) adhesion classification; (Figure S6) paxillin images; (Figure S7) different adhesion types in proximity; (Figure S8) E-cadherin staining of adhesions; (Figure S9) image analysis pipeline; (Figure S10) drug treatment with sub-kPa substrates; (Figure S11) blebbistatin treatment; (Table S1) references for cell elasticities (PDF)

## AUTHOR INFORMATION

### Corresponding Author

Venkat Maruthamuthu – Department of Mechanical & Aerospace Engineering, Old Dominion University, Norfolk, Virginia 23529, United States; [orcid.org/0000-0002-3470-5274](https://orcid.org/0000-0002-3470-5274); Email: [vmarutha@odu.edu](mailto:vmarutha@odu.edu)

### Authors

Mohamad Eftekharijoo – Department of Mechanical & Aerospace Engineering, Old Dominion University, Norfolk, Virginia 23529, United States

Mazen Mezher – Department of Mechanical & Aerospace Engineering, Old Dominion University, Norfolk, Virginia 23529, United States

Siddharth Chatterji – Department of Mechanical & Aerospace Engineering, Old Dominion University, Norfolk, Virginia 23529, United States

Complete contact information is available at:

<https://pubs.acs.org/10.1021/acsbmaterials.2c00253>

### Author Contributions

<sup>†</sup>M.E. and M.M. contributed equally to this work.

### Author Contributions

V.M. designed the research. M.E., M.M., and S.C. performed the research. M.E., M.M., and V.M. analyzed the data. V.M. wrote the paper.

### Notes

The authors declare no competing financial interest.

## ACKNOWLEDGMENTS

We thank Guijun Wang and Pooja Sharma for assistance with rheology measurements. We thank Allen Ehrlicher for useful discussion on soft silicone substrates. We thank Wei Cao at the ODU Applied Research Center at Newport News, VA for assistance with SEM. The web app PlotsOfData<sup>66</sup> was used to render the plot in Figure 2. V.M. acknowledges support from the National Institutes of Health under award number 2R15GM116082.

## REFERENCES

- Meng, W.; Takeichi, M. Adherens junction: molecular architecture and regulation. *Cold Spring Harbor Perspect. Biol.* **2009**, *1*, No. a002899.
- Gumbiner, B. M. Regulation of cadherin-mediated adhesion in morphogenesis. *Nat. Rev. Mol. Cell Biol.* **2005**, *6*, 622–634.
- Wu, Y.; Jin, X.; Harrison, O.; Shapiro, L.; Honig, B. H.; Ben-Shaul, A. Cooperativity between trans and cis interactions in cadherin-



mediated junction formation. *Proc. Natl. Acad. Sci. U. S. A.* **2010**, *107*, 17592–17597.

(4) Brieher, W. M.; Yap, A. S. Cadherin junctions and their cytoskeleton(s). *Curr. Opin. Cell Biol.* **2013**, *25*, 39–46.

(5) Maitre, J.; Berthoumieux, H.; Krens, S. F. G.; Salbreux, G.; Jülicher, F.; Paluch, E.; Heisenberg, C. P. Adhesion Functions in Cell Sorting by Mechanically Coupling the Cortices of Adhering Cells. *Science* **2012**, *338*, 253–256.

(6) Yap, A.; Liang, X.; Gomez, G. Current perspectives on cadherin-cytoskeleton interactions and dynamics. *Cell Health Cytoskeleton* **2015**, *11*.

(7) Charras, G.; Yap, A. S. Tensile Forces and Mechanotransduction at Cell-Cell Junctions. *Curr. Biol.* **2018**, *28*, R445–R457.

(8) Kechagia, J. Z.; Ivaska, J.; Roca-Cusachs, P. Integrins as biomechanical sensors of the microenvironment. *Nat. Rev. Mol. Cell Biol.* **2019**, *20*, 457–473.

(9) Bershadsky, A. D.; Balaban, N. Q.; Geiger, B. Adhesion-dependent cell mechanosensitivity. *Annu. Rev. Cell Dev. Biol.* **2003**, *19*, 677–695.

(10) Liu, Z.; Tan, J. L.; Cohen, D. M.; Yang, M. T.; Sniadecki, N. J.; Ruiz, S. A.; Nelson, C. M.; Chen, C. S. Mechanical tugging force regulates the size of cell-cell junctions. *Proc. Natl. Acad. Sci. U. S. A.* **2010**, *107*, 9944–9949.

(11) Yonemura, S.; Wada, Y.; Watanabe, T.; Nagafuchi, A.; Shibata, M. alpha-Catenin as a tension transducer that induces adherens junction development. *Nat. Cell Biol.* **2010**, *12*, 533–542.

(12) Ishiyama, N.; Sarpal, R.; Wood, M. N.; Barrick, S. K.; Nishikawa, T.; Hayashi, H.; Kobb, A. B.; Flozak, A. S.; Yemelyanov, A.; Fernandez-Gonzalez, R.; Yonemura, S.; Leckband, D. E.; Gottardi, C. J.; Tepass, U.; Ikura, M. Force-dependent allostery of the alpha-catenin actin-binding domain controls adherens junction dynamics and functions. *Nat. Commun.* **2018**, *9*, 5121.

(13) Lecuit, T.; Lenne, P.-F.; Munro, E. Force Generation, Transmission, and Integration during Cell and Tissue Morphogenesis. *Annu. Rev. Cell Dev. Biol.* **2011**, *27*, 157–184.

(14) Kumar, S.; Weaver, V. M. Mechanics, malignancy, and metastasis: the force journey of a tumor cell. *Cancer Metastasis Rev.* **2009**, *28*, 113–127.

(15) Wagh, A. A.; Roan, E.; Chapman, K. E.; Desai, L. P.; Rendon, D. A.; Eckstein, E. C.; Waters, C. M. Localized elasticity measured in epithelial cells migrating at a wound edge using atomic force microscopy. *Am. J. Phys. Lung Cell Mol. Phys.* **2008**, *295*, L54–L60.

(16) Bruner, H. C.; Derksen, P. W. B. Loss of E-Cadherin-Dependent Cell-Cell Adhesion and the Development and Progression of Cancer. *Cold Spring Harbor Perspect. Biol.* **2018**, *10*, No. a029330.

(17) Petrova, Y. I.; Schecterson, L.; Gumbiner, B. M. Roles for E-cadherin cell surface regulation in cancer. *Mol. Biol. Cell* **2016**, *27*, 3233–3244.

(18) Alibert, C.; Goud, B.; Manneville, J. B. Are cancer cells really softer than normal cells? *Biol. Cell* **2017**, *109*, 167–189.

(19) Cross, S. E.; Jin, Y. S.; Rao, J.; Gimzewski, J. K. Nanomechanical analysis of cells from cancer patients. *Nat. Nanotechnol.* **2007**, *2*, 780–783.

(20) Xu, W.; Mezencev, R.; Kim, B.; Wang, L.; McDonald, J.; Sulchek, T. Cell stiffness is a biomarker of the metastatic potential of ovarian cancer cells. *PLoS One* **2012**, *7*, No. e46609.

(21) Prabhune, M.; Belge, G.; Dotzauer, A.; Bullerdiek, J.; Radmacher, M. Comparison of mechanical properties of normal and malignant thyroid cells. *Micron* **2012**, *43*, 1267–1272.

(22) Faria, E. C.; Ma, N.; Gazi, E.; Gardner, P.; Brown, M.; Clarke, N. W.; Snook, R. D. Measurement of elastic properties of prostate cancer cells using AFM. *Analyst* **2008**, *133*, 1498–1500.

(23) Ciepmans, B. N.; van Ijzendoorn, S. C. Epithelial cell-cell junctions and plasma membrane domains. *Biochim. Biophys. Acta* **2009**, *1788*, 820–831.

(24) Lambert, M.; Padilla, F.; Mege, R. M. Immobilized dimers of N-cadherin-Fc chimera mimic cadherin-mediated cell contact formation: contribution of both outside-in and inside-out signals. *J. Cell Sci.* **2000**, *113*, 2207–2219.

(25) McLachlan, R. W.; Kraemer, A.; Helwani, F. M.; Kovacs, E. M.; Yap, A. S. E-cadherin adhesion activates c-Src signaling at cell-cell contacts. *Mol. Biol. Cell* **2007**, *18*, 3214–3223.

(26) Borghi, N.; Lowndes, M.; Maruthamuthu, V.; Gardel, M. L.; Nelson, W. J. Regulation of cell motile behavior by crosstalk between cadherin- and integrin-mediated adhesions. *Proc. Natl. Acad. Sci.* **2010**, *107*, 13324–13329.

(27) Maruthamuthu, V.; Gardel, M. L. Protrusive activity guides changes in cell-cell tension during epithelial cell scattering. *Biophys. J.* **2014**, *107*, 555–563.

(28) Suffoletto, K.; Jetta, D.; Hua, S. Z. E-cadherin mediated lateral interactions between neighbor cells necessary for collective migration. *J. Biomech.* **2018**, *71*, 159–166.

(29) Kovacs, E. M.; Ali, R. G.; McCormack, A. J.; Yap, A. S. E-cadherin homophilic ligation directly signals through Rac and phosphatidylinositol 3-kinase to regulate adhesive contacts. *J. Biol. Chem.* **2002**, *277*, 6708–6718.

(30) Cavey, M.; Rauzi, M.; Lenne, P. F.; Lecuit, T. A two-tiered mechanism for stabilization and immobilization of E-cadherin. *Nature* **2008**, *453*, 751–756.

(31) Collins, C.; Denisin, A. K.; Pruitt, B. L.; Nelson, W. J. Changes in E-cadherin rigidity sensing regulate cell adhesion. *Proc. Natl. Acad. Sci. U. S. A.* **2017**, *114*, E5835–E5844.

(32) Yang, Y.-A.; Nguyen, E.; Narayana, G. H. N. S.; Heuzé, M.; Fu, C.; Yu, H.; Mège, R.-M.; Ladoux, B.; Sheetz, M. P. Local contractions regulate E-cadherin rigidity sensing. *Sci. Adv.* **2022**, *8*, No. eabk0387.

(33) Ladoux, B.; Anon, E.; Lambert, M.; Rabodzey, A.; Hersen, P.; Buguin, A.; Silberzan, P.; Mège, R. M. Strength dependence of cadherin-mediated adhesions. *Biophys. J.* **2010**, *98*, 534–542.

(34) Collins, T. J. ImageJ for microscopy. *BioTechniques* **2007**, *43*, 25–30.

(35) Carpenter, A. E.; Jones, T. R.; Lamprecht, M. R.; Clarke, C.; Kang, I. H.; Friman, O.; Guertin, D. A.; Chang, J. H.; Lindquist, R. A.; Moffat, J.; Golland, P.; Sabatini, D. M. CellProfiler: image analysis software for identifying and quantifying cell phenotypes. *Genome Biol.* **2006**, *7*, R100.

(36) Prakasam, A. K.; Maruthamuthu, V.; Leckband, D. E. Similarities between heterophilic and homophilic cadherin adhesion. *Proc. Natl. Acad. Sci. U. S. A.* **2006**, *103*, 15434–15439.

(37) Drees, F.; Reilein, A.; Nelson, W. J. Cell Adhesion Assays: Fabrication of an E-cadherin Substratum and Isolation of Lateral and Basal Membrane Patches. *Methods Mol. Biol.* **2004**, *294*, 303–320.

(38) Hinck, L.; Näthke, I. S.; Papkoff, J.; Nelson, W. J. Dynamics of cadherin/catenin complex formation: novel protein interactions and pathways of complex assembly. *J. Cell Biol.* **1994**, *125*, 1327–1340.

(39) Muhamed, I.; Wu, J.; Sehgal, P.; Kong, X.; Tajik, A.; Wang, N.; Leckband, D. E. E-cadherin-mediated force transduction signals regulate global cell mechanics. *J. Cell Sci.* **2016**, *129*, 1843–1854.

(40) Wu, P. H.; Aroush, D. R.; Asnacios, A.; Chen, W. C.; Dokukin, M. E.; Doss, B. L.; Durand-Smet, P.; Ekpenyong, A.; Guck, J.; Guz, N. V.; Janmey, P. A.; Lee, J. S. H.; Moore, N. M.; Ott, A.; Poh, Y. C.; Ros, R.; Sander, M.; Sokolov, I.; Staunton, J. R.; Wang, N.; Whyte, G.; Wirtz, D. A comparison of methods to assess cell mechanical properties. *Nat. Methods* **2018**, *15*, 491–498.

(41) Li, Y.; Schnekenburger, J.; Duits, M. H. G. Intracellular particle tracking as a tool for tumor cell characterization. *J. Biomed. Opt.* **2009**, *14*, No. 064005.

(42) Lekka, M.; Laidler, P.; Gil, D.; Lekki, J.; Stachura, Z.; Hryniewicz, A. Z. Elasticity of normal and cancerous human bladder cells studied by scanning force microscopy. *Eur. Biophys. J.* **1999**, *28*, 312.

(43) Omidvar, R.; Tafazzoli-shadpour, M.; Shokrgozar, M. A.; Rostami, M. Atomic force microscope-based single cell force spectroscopy of breast cancer cell lines: An approach for evaluating cellular invasion. *J. Biomech.* **2014**, *47*, 3373–3379.

(44) Bastatas, L.; Martinez-Marin, D.; Matthews, J.; Hashem, J.; Lee, Y. J.; Sennoune, S.; Filleur, S.; Martinez-Zaguilan, R.; Park, S. AFM nano-mechanics and calcium dynamics of prostate cancer cells with

distinct metastatic potential. *Biochim. Biophys. Acta, Gen. Subj.* **2012**, *1820*, 1111–1120.

(45) Ramos, J. R.; Pabijan, J.; Garcia, R.; Lekka, M. The softening of human bladder cancer cells happens at an early stage of the malignancy process. *Beilstein J. Nanotechnol.* **2014**, *5*, 447–457.

(46) Rebelo, L. M.; de Sousa, J. S.; Filho, J. M.; Radmacher, M. Comparison of the viscoelastic properties of cells from different kidney cancer phenotypes measured with atomic force microscopy. *Nanotechnology* **2013**, *24*, No. 055102.

(47) le Duc, Q.; Shi, Q.; Blonk, I.; Sonnenberg, A.; Wang, N.; Leckband, D.; de Rooij, J. Vinculin potentiates E-cadherin mechanosensing and is recruited to actin-anchored sites within adherens junctions in a myosin II-dependent manner. *J. Cell Biol.* **2010**, *189*, 1107–1115.

(48) Timoshenko, S.; Goodier, J. N., *Theory of elasticity*. McGraw-Hill: New York, 1970.

(49) Xu, Q.; Jensen, K. E.; Boltyanskiy, R.; Sarfati, R.; Style, R. W.; Dufresne, E. R. Direct measurement of strain-dependent solid surface stress. *Nat. Commun.* **2017**, *8*, 555.

(50) Style, R. W.; Boltyanskiy, R.; German, G. K.; Hyland, C.; MacMinn, C. W.; Mertz, A. F.; Wilen, L. A.; Xu, Y.; Dufresne, E. R. Traction force microscopy in physics and biology. *Soft Matter* **2014**, *10*, 4047–4055.

(51) Alcaraz, J.; Buscemi, L.; Grabulosa, M.; Trepas, X.; Fabry, B.; Farré, R.; Navajas, D. Microrheology of Human Lung Epithelial Cells Measured by Atomic Force Microscopy. *Biophys. J.* **2003**, *84*, 2071–2079.

(52) Mikolaszek, B.; Kazlauske, J.; Larsson, A.; Sznitowska, M. Controlled Drug Release by the Pore Structure in Polydimethylsiloxane Transdermal Patches. *Polymers* **2020**, *12*, 1520.

(53) Ferreira, P.; Carvalho, Á.; Correia, T. R.; Antunes, B. P.; Correia, I. J.; Alves, P. Functionalization of polydimethylsiloxane membranes to be used in the production of voice prostheses. *Sci. Technol. Adv. Mater.* **2013**, *14*, No. 055006.

(54) Cohen, D. J.; Gloerich, M.; Nelson, W. J. Epithelial self-healing is recapitulated by a 3D biomimetic E-cadherin junction. *Proc. Natl. Acad. Sci. U. S. A.* **2016**, *113*, 14698–14703.

(55) Hotulainen, P.; Lappalainen, P. Stress fibers are generated by two distinct actin assembly mechanisms in motile cells. *J. Cell Biol.* **2006**, *173*, 383–394.

(56) Bubb, M. R.; Senderowicz, A. M.; Sausville, E. A.; Duncan, K. L.; Korn, E. D. Jasplakinolide, a cytotoxic natural product, induces actin polymerization and competitively inhibits the binding of phalloidin to F-actin. *J. Biol. Chem.* **1994**, *269*, 14869–14871.

(57) Holzinger, A. Jasplakinolide. An actin-specific reagent that promotes actin polymerization. *Methods Mol. Biol.* **2000**, *161*, 109–120.

(58) Cramer, L. P. Role of actin-filament disassembly in lamellipodium protrusion in motile cells revealed using the drug jasplakinolide. *Curr. Biol.* **1999**, *9*, 1095–1105.

(59) Shewan, A. M.; Maddugoda, M.; Kraemer, A.; Stehbins, S. J.; Verma, S.; Kovacs, E. M.; Yap, A. S. Myosin 2 Is a Key Rho Kinase Target Necessary for the Local Concentration of E-Cadherin at Cell-Cell Contacts. *Mol. Biol. Cell* **2005**, *16*, 4531–4542.

(60) Zigmond, S. H. Formin-induced nucleation of actin filaments. *Curr. Opin. Cell Biol.* **2004**, *16*, 99–105.

(61) Rizvi, S. A.; Neidt, E. M.; Cui, J.; Feiger, Z.; Skau, C. T.; Gardel, M. L.; Kozmin, S. A.; Kovar, D. R. Identification and characterization of a small molecule inhibitor of formin-mediated actin assembly. *Chem. Biol.* **2009**, *16*, 1158–1168.

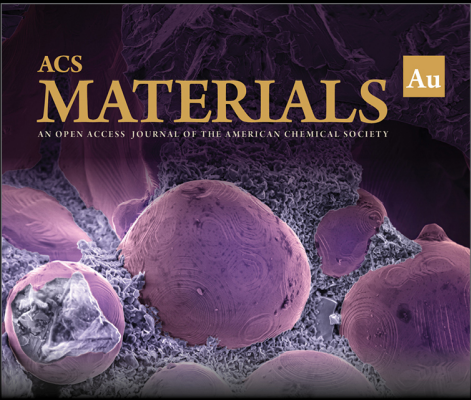
(62) Carramusa, L.; Ballestrin, C.; Zilberman, Y.; Bershadsky, A. D. Mammalian diaphanous-related formin Dia1 controls the organization of E-cadherin-mediated cell-cell junctions. *J. Cell Sci.* **2007**, *120*, 3870–3882.

(63) Nishimura, Y.; Shi, S.; Zhang, F.; Liu, R.; Takagi, Y.; Bershadsky, A. D.; Viasnoff, V.; Sellers, J. R. The formin inhibitor SMIFH2 inhibits members of the myosin superfamily. *J. Cell Sci.* **2021**, *134* (), DOI: 10.1242/jcs.253708.

(64) Watanabe, T.; Sato, K.; Kaibuchi, K. Cadherin-mediated intercellular adhesion and signaling cascades involving small GTPases. *Cold Spring Harbor Perspect. Biol.* **2009**, *1*, No. a003020.

(65) Yamada, S.; Nelson, W. J. Localized zones of Rho and Rac activities drive initiation and expansion of epithelial cell–cell adhesion. *J. Cell Biol.* **2007**, *178*, 517–527.


(66) Postma, M.; Goedhart, J. PlotsOfData-A web app for visualizing data together with their summaries. *PLoS Biol.* **2019**, *17*, No. e3000202.




ACS  
**MATERIALS** Au  
AN OPEN ACCESS JOURNAL OF THE AMERICAN CHEMICAL SOCIETY

Editor-in-Chief: **Prof. Shelley D. Minteer**, University of Utah, USA

Deputy Editor:  
**Prof. Stephanie L. Brock**  
Wayne State University, USA

**Open for Submissions** 

pubs.acs.org/materialsau  ACS Publications  
Most Trusted. Most Cited. Most Read.